EUROfusion

Microscopy investigation and assessment of mechanical properties of Langmuir probes

Elżbieta Fortuna-Zaleśna[1], Maciej Spychalski[1], Anna Widdowson[2], Robert Kerr[2] and Marek Rubel[3]

[1]Warsaw University of Technology
[2]CCFCE, Culham Science Centre, Abingdon
[3]KTH Royal Institute of Technology

This work has been carried out within the framework of the EUROfusion Consortium, funded by the European Union via the Euratom Research and Training Programme (Grant Agreement No 101052200 — EUROfusion). Views and opinions expressed are however those of the author(s) only and do not necessarily reflect those of the European Union or the European Commission. Neither the European Union nor the European Commission can be held responsible for them.

Outlook

- Examined material
- Principles of NIT
- Probes location in JET
- Surface morphology of examined probes
- Grain size assessment
- Surface development
- Nano mechanical properties
- Further plans

Langmuir probes

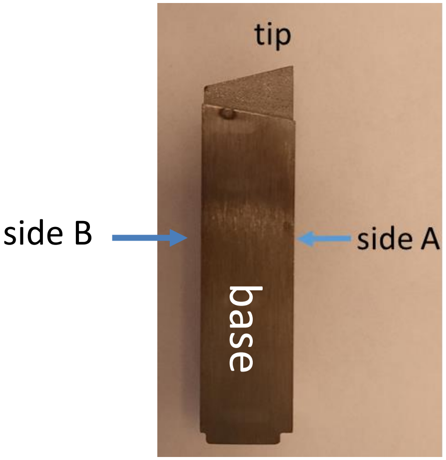

Material:
Three probes designated as LP 1, 3 and 5 removed from Module 16W, Tile 5, in 2015, after ILW-2 (probe 1 mounted at stack A, probes 3 and 5 at stack B). <u>All probes have the same geometry.</u>

Experimental procedure:
When examining the probes, we utilize the procedure successfully implemented when examining the probes removed after the second ILW campaign and presented in the work M. Spychalski et al. „Tungsten Langmuir probes from JET-with the ITER-Like Wall: Assessment of mechanical properties by nano-indentation”, Phys. Scr. 96 (2021) 124072.

Mechanical properties were determined by nanoindentation using a Hysitron Ti-900 triboindenter, while surface development was examined by optical profilometer Veeco NT9300. Because of the small dimensions of the tip, the force applied was 10 mN. Due to the large development of the surface, it was imaged in the SPM mode before and after each measurement. Only measurements resulting in regular imprints are included.

The nano-hardness measurements were carried out in four regions of LP-5: in the tip and the base, at two sides A and B, and in two regions of probe LP-1, at side A, in the tip and the base.

NIT principles

- NIT meets the needs of technological development related to component miniaturization, development of surface engineering techniques, composite materials, and polymers. Its potential has been demonstrated in the characterization of W surfaces irradiated by heavy ions, hydrogen, or helium plasmas.

- The method was developed in the early 1980’ to measure the hardness and elastic modulus of materials from indentation force-displacement curves obtained during one cycle of loading and unloading (method developed by Doerner and Nix, later improved by Oliver and Pharr).

- The material hardness in the case of nanoindentation is calculated from the formula:

$$H = \frac{P_{max}}{A(h_c)}$$

where: P_{max} is the maximum force and A (h_c)— is the projected contact area at that maximum load.

The value of A (h_c) can be determined on the basis of the so-called shape function of the indenter. For an ideal sharp Berkovich triangular pyramid indenter, the contact area A is given by the formula:

$$A = 24.56\, h_c^2$$

NIT principles

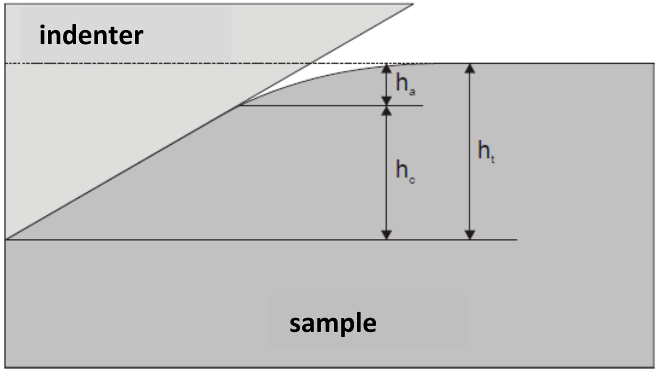

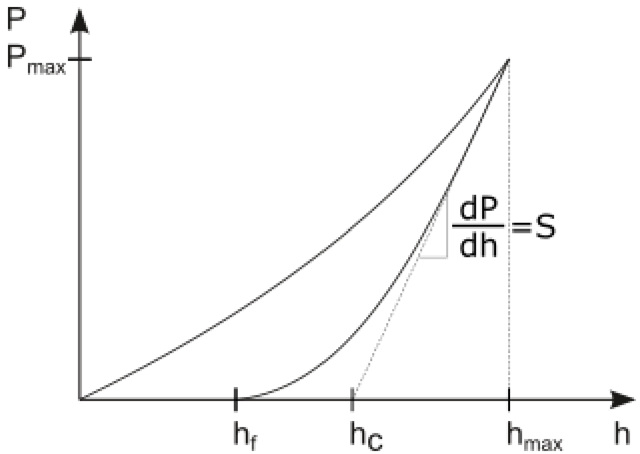

A schematic force-displacement curve for nano-indentation obtained in one cycle of loading and unloading for elastic-plastic material

where:

h_f - the final depth of penetration after unloading,

h_c -contact depth during maximum load,

h_{max}- the maximum displacement,

S - the contact stiffness (the slope of the upper portion of the unloading curve).

The value of A(hc) is determined indirectly through the determination of contact stiffness (S) of the indenter-specimen during unloading.

$$h_c = h_{max} - 0{,}75 * \frac{P_{max}}{S}$$

Probes location in JET

Langmuir probes arrays in the JET-ILW divertor; Tile numbers are indicated.

a) b) c)

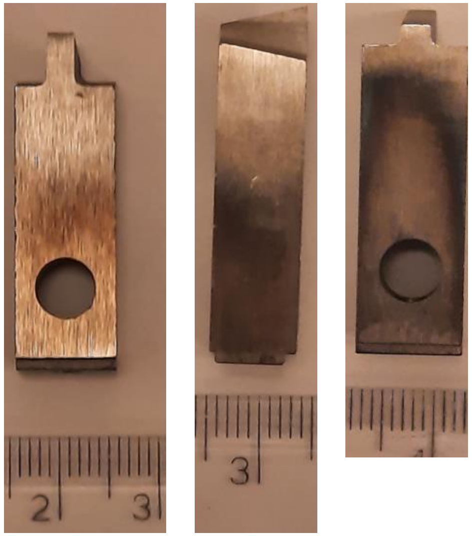

Images of the LP-5: a) side A, b) side wall, c) side B.

- *Visible longitudinal lines from grinding, screw hole, and dark areas corresponding to thin deposits.*
- *The colour change is not observed on the tip and just below it.*
- *The probe is attached to the plate from side B.*

Surface morphology, probe 5

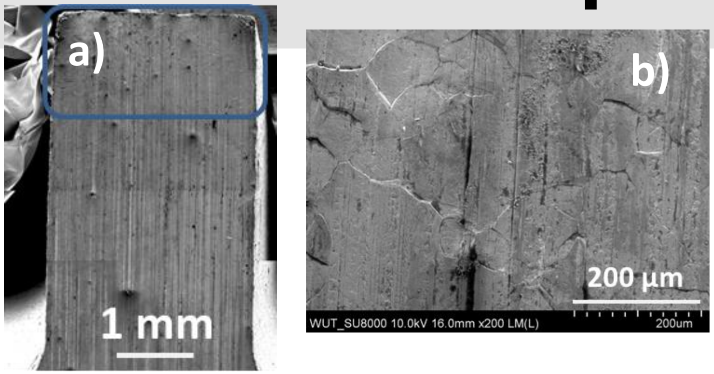

SEM images of the tip (a) and the tip end morphology (b), side A. *Grain boundaries are well visible. Recrystallized zone.*

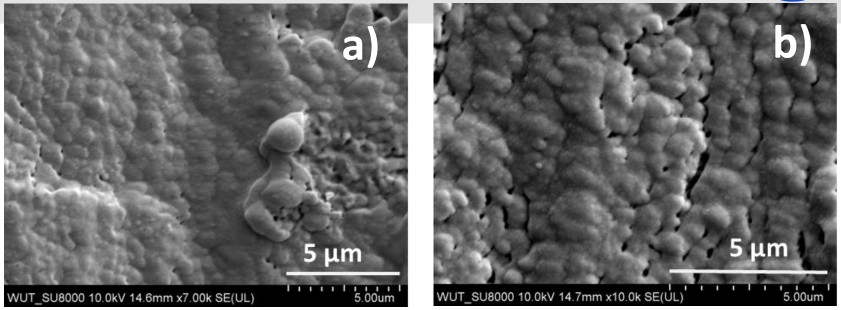

SEM images of the tip part below the re-crystalized zone. *Overheated area.*

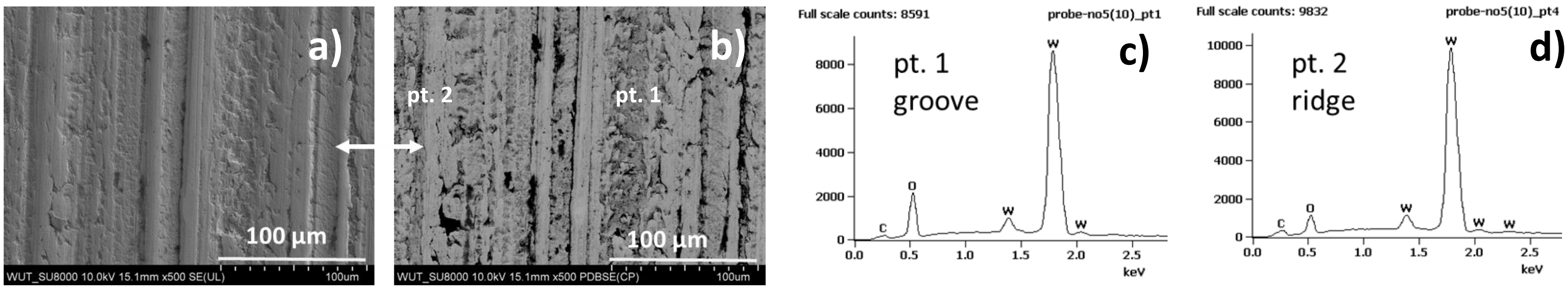

SEM images of the base morphology (a-b) together with the corresponding EDX spectra (c-d). *Contrast differences visible in the images registered in the BSE mode indicate redeposition in the grooves.*

- *Tip*
  - ✓ *Large re-crystalized zone near the tip end, ˜1.3 mm.*
  - ✓ *Overheated material with visible pores below the re-crystallized part. Locally re-solidified droplets were found.*
- *Base*
  - ✓ *No signs of re-melting,*
  - ✓ *Re-deposition present (contrast changes visible in the images registered in the BSE mode; darker contrast areas cover/overlap with the grooves).*

Surface morphology, probe 1, tip

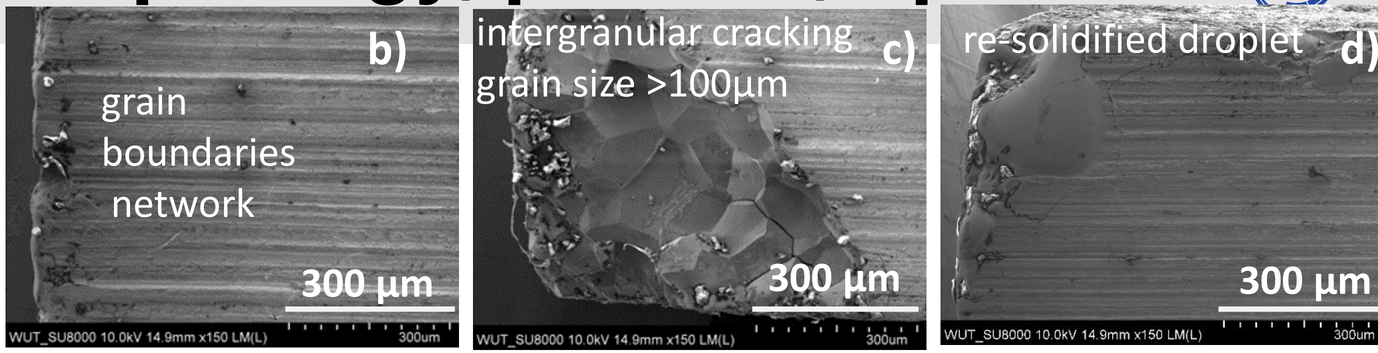

SEM images of the tip (a) and the tip end (b-d).

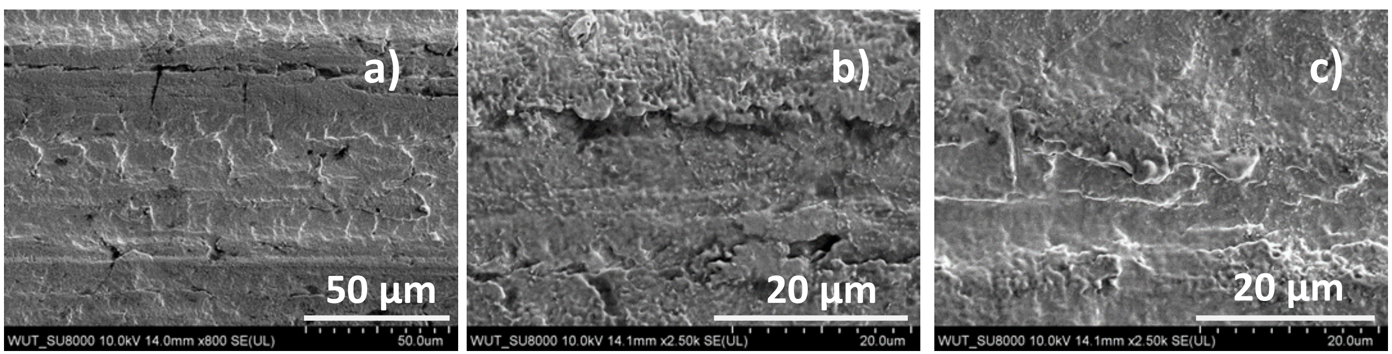

SEM images of the tip upper part morphology. *Damage in the upper part of the tip was found. Cracks and surface re-melting. Damage is limited to the top zone of the tip.*

Surface morphology, probe 1, base

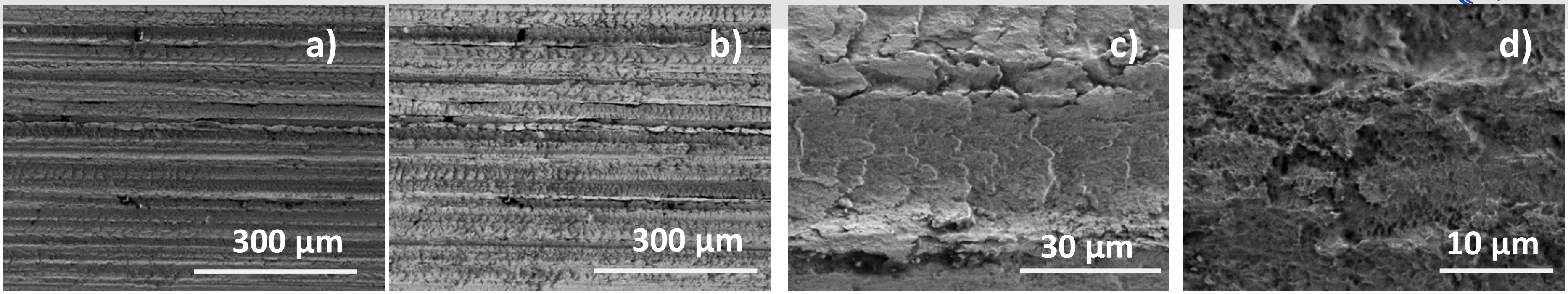

SEM images of the base morphology. *No signs of re-melting. Re-deposition.*

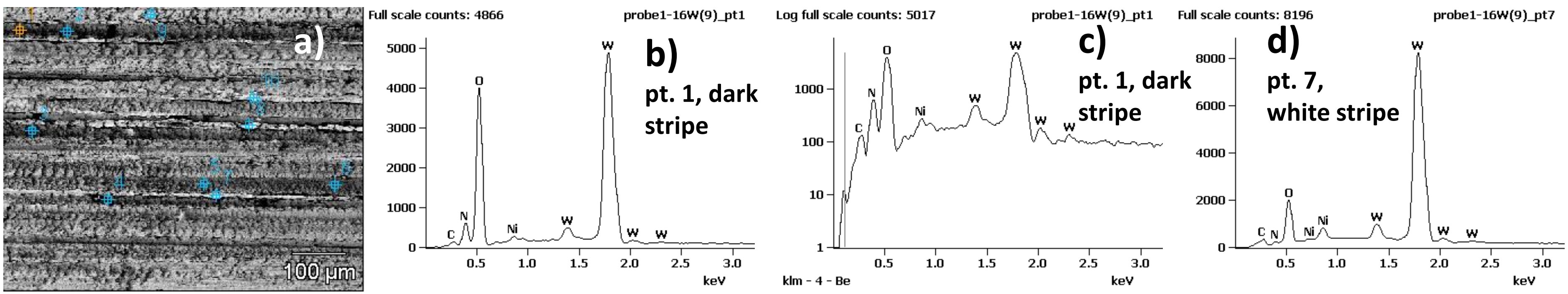

SEM image of the base together with corresponding EDX spectra. *In the grooves higher signals from oxygen and nitrogen.*

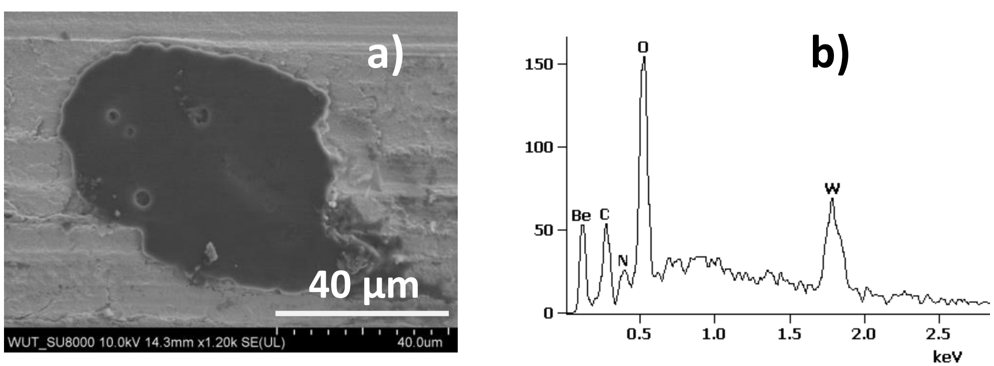

SEM image of the Be splash (a) found under the tip together with the corresponding EDX spectrum (b).

Grain size estimation on FIB cross-section, LP-5, side B, base

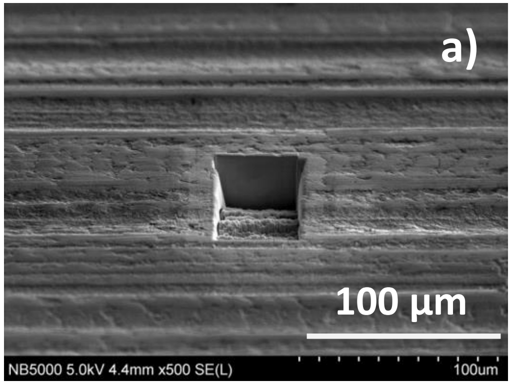

SEM images of the FIB cross-section, LP-5, side A, base.

- *In order to determine the grain size of the material, a FIB cross-section (30 µm x 20 µm) was made on LP-5.*
- *At the surface, a zone of plastic deformation with a thickness of ca. 3 µm was revealed.*
- *The grains visible on the cross-section are approx. 10 µm in* size *(note: the grain size determined on probe 8 located at plate 3 in the tip area -different geometry - was 33um, metallographic examination, see R. Kerr's presentation – WP PWIE 2022 Review Meeting, 20-10-2022).*

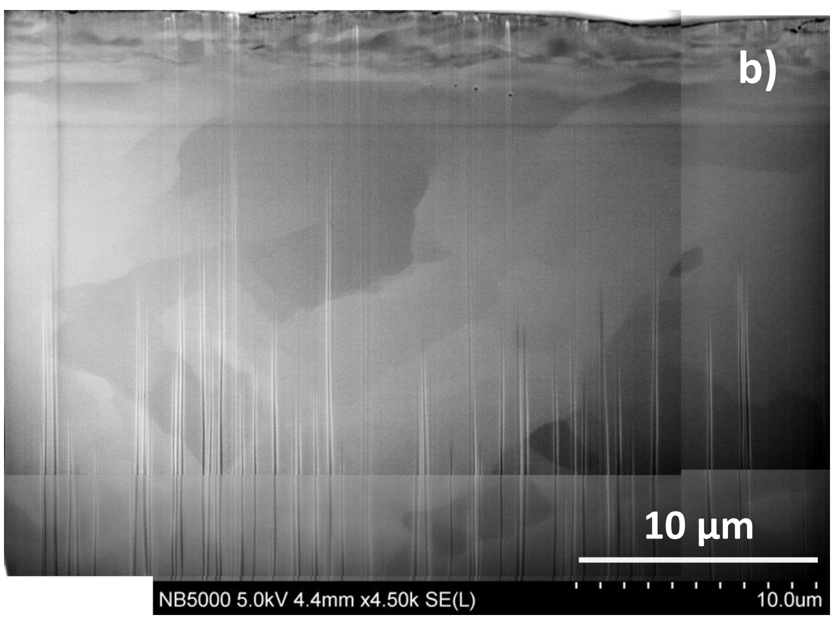

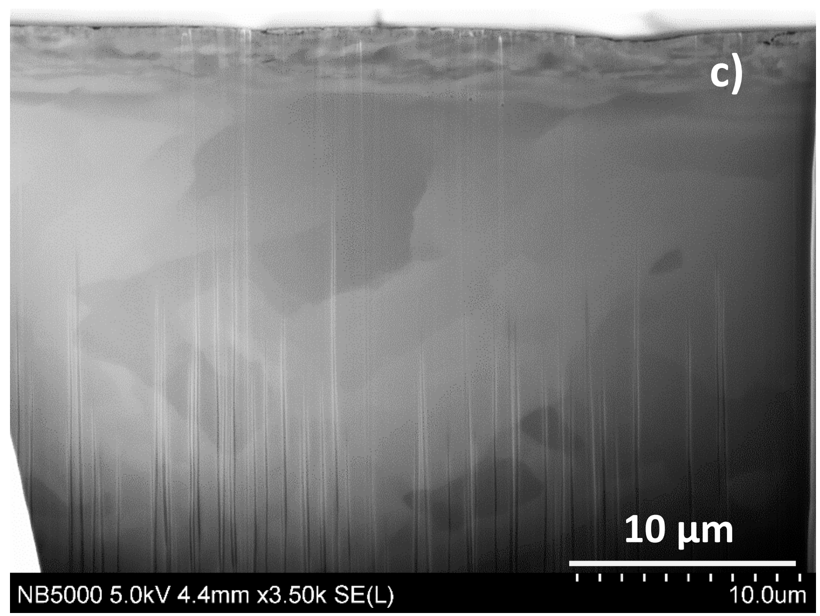

Surface development

Results of surface development measurements at side A of the probes

(*mag. 11.5x, Ra was calculated from five areas with dimensions equal to 412×550 µm²*)

Roughness average, Ra [µm]			
Probe 1		Probe 5	
tip	base	tip	base
1.4 ± 0.18	**1.33 ± 0.12**	**1.11 ± 0.09**	**1.04 ± 0.14**

The study has revealed that the roughness values for the tip and the base, for both probes are at the same level. However, the roughness of LP-1 is higher than that of LP-5.

Exemplary images of the surface development in the base, side A: (a) LP-1 and (b) LP-5.

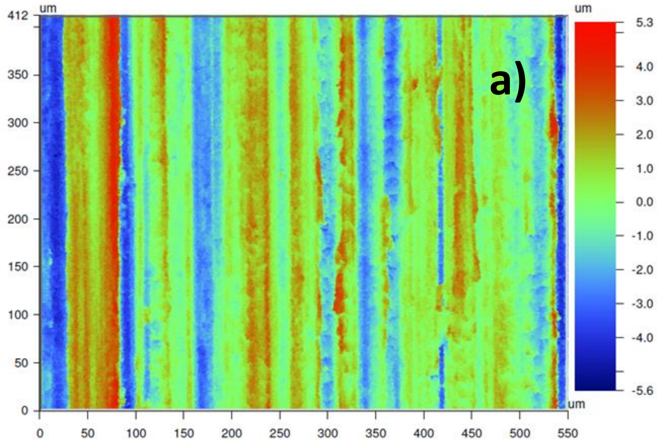

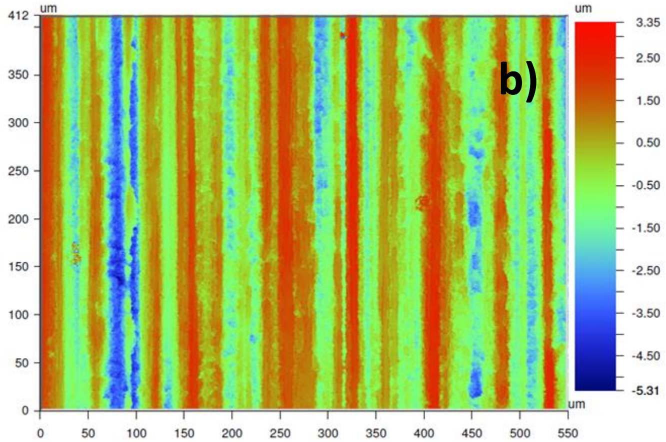

Surface imaging in the SPM mode

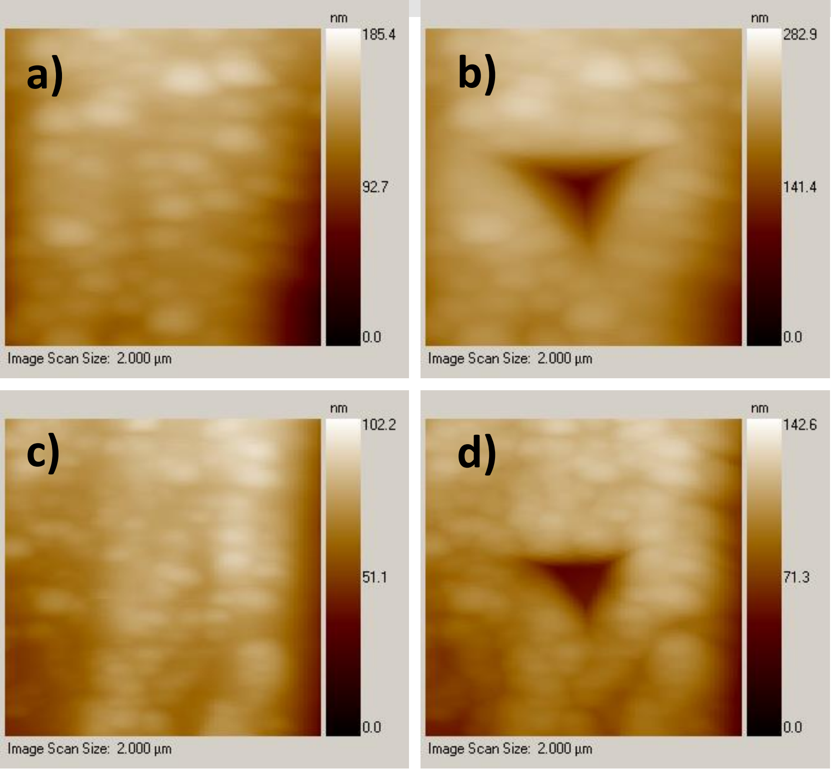

SPM images of the probe surface before the measurement and of the imprint made on the recorded area, for the tip (a-b) and the base (c-d), LP-5, side A.

The imprint from the tip area is larger and deeper.

The roughness calculated from the SPM images (projected area 4 µm^2) was 14 and 19 nm for the tip and the base of LP-1, respectively.
For LP-5, the values determined for the tip and the base were at the comparable level of 13 nm.

Results of surface development measurements

Roughness average, Ra [nm]					
Probe 1		Probe 5A		Probe 5B	
tip	base	tip	base	tip	base
14 ± 9	**19 ± 3**	**13 ± 5**	**13 ± 3**	**11 ± 4**	**11 ± 4**

Nanomechnical properties

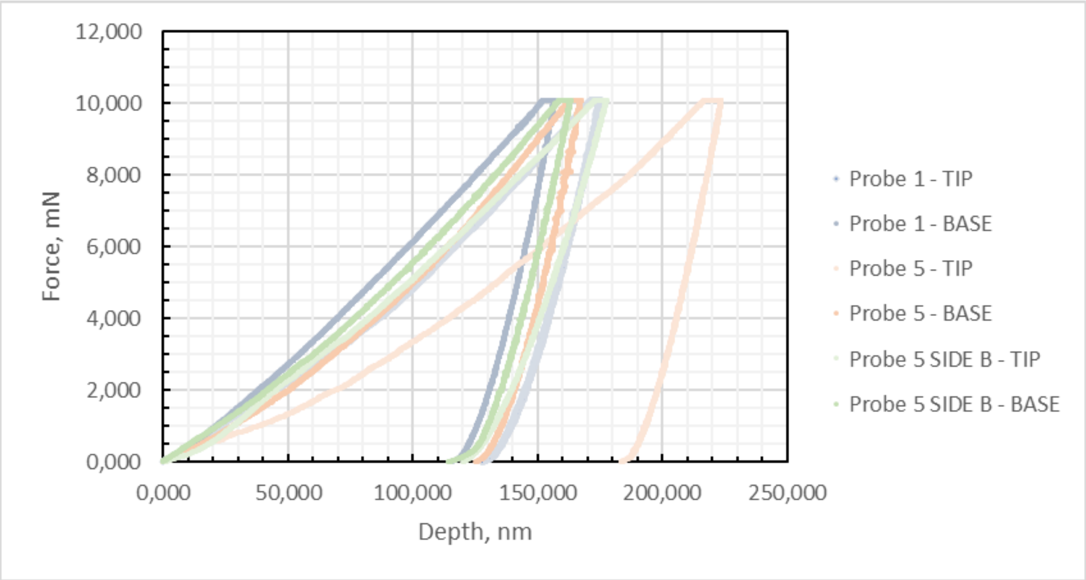

Comparison of force-depth curves for all examined zones.
The only curve that stands out from the others is the one obtained on side A of the LP-5 tip.

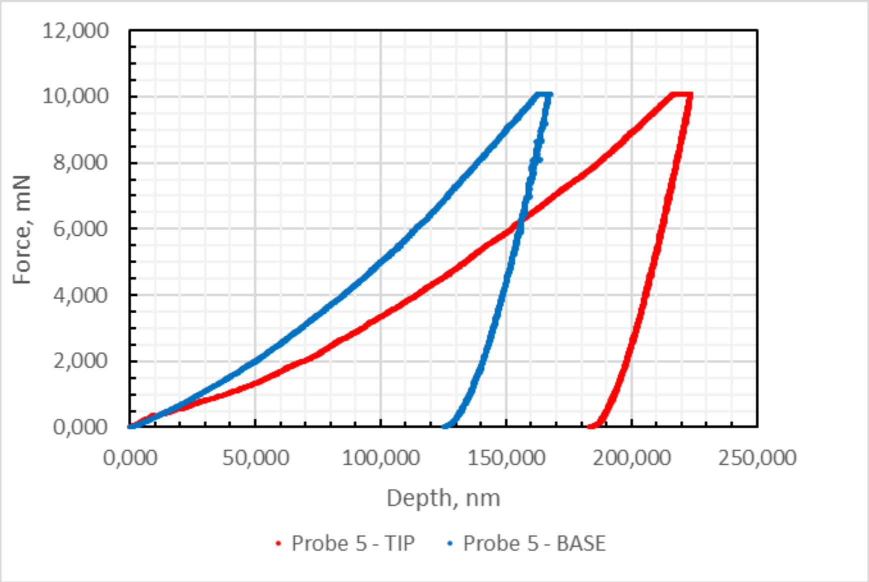

Comparison of force-depth curves for tip and base of LP-5, side A.
On the tip, the indenter penetrates much deeper than on the base.

Nanomechanical properties

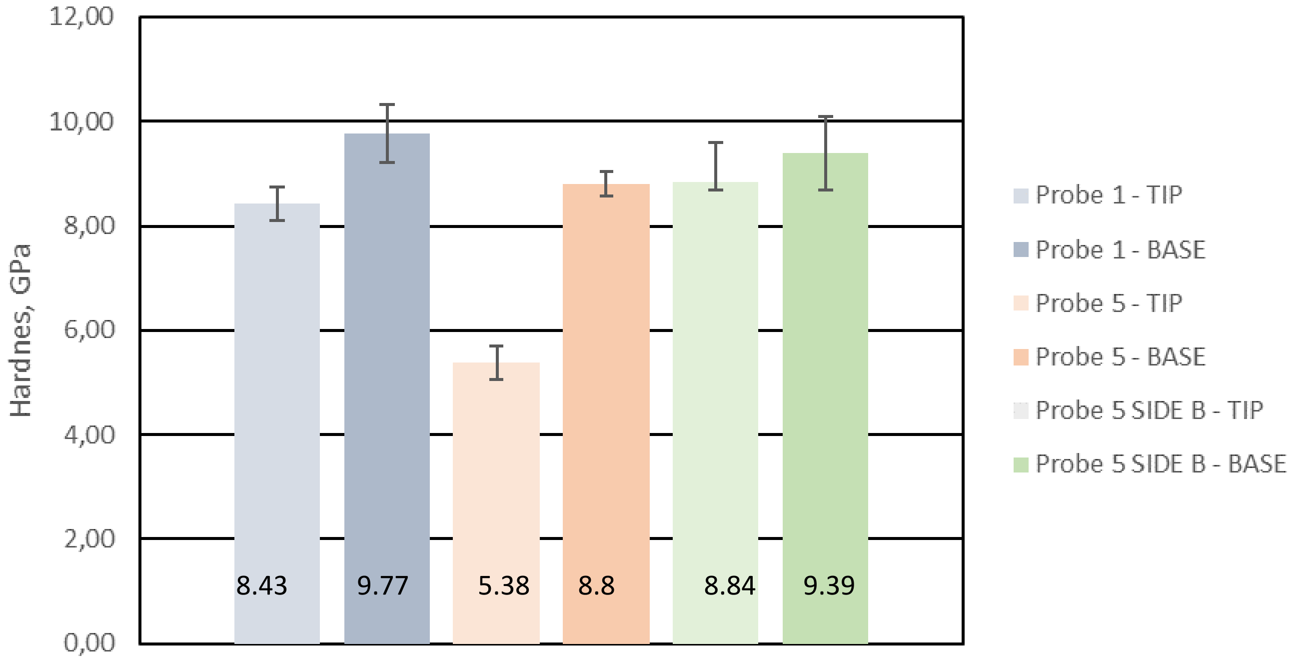

Results of nanohardness measurements in the LP-5 and LP-1.

- *The most important result is the large difference in the hardness value in the tip and the base of LP-5 at side A, 5.4 GPa versus 8.8 GPa, respectively. The hardness values measured on the base and tip on the B-side were similar to those measured on the base on the A-side.*

- *The differences in hardness on the base and tip of probe 1, measured on the A-side, were small, which is expected considering the fact that the probe was placed next to stack A.*

Unexposed probe

Image of an unexposed probe.

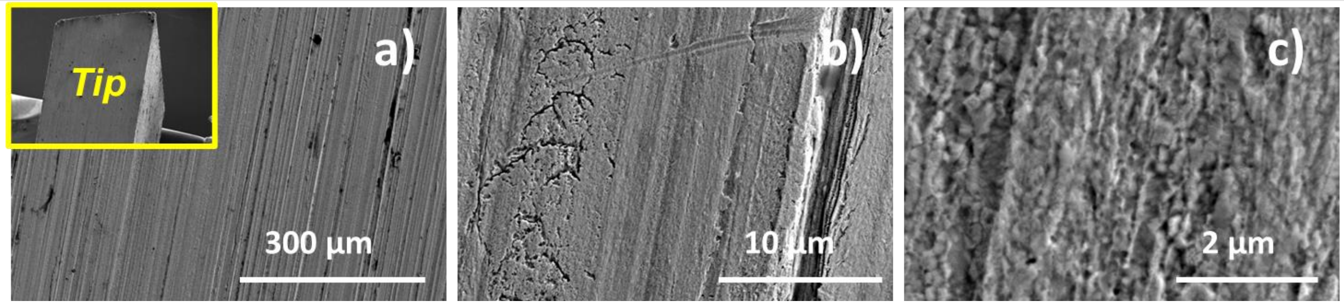

SEM images of the unexposed probe surface in the tip part. *The same morphology as observed on the base of probes LP-1 and LP-5.*

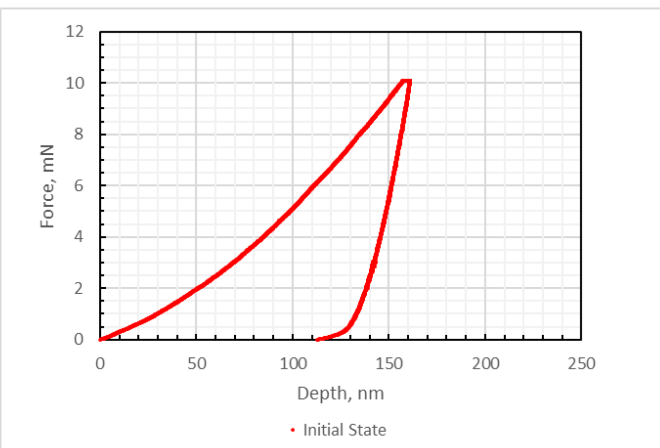

Force-depth curves for the base of the unexposed probe. *The same shape as for LP-1 and LP-5 (except the LP-5A tip).*

Results of nano-hardness and surface development measurements

H	8.5 GPa
Ra (for mag. 11.5 x)	340 nm
Ra (*projected area 4 µm²)*	11 nm

Conclusion

- *This work has provided information both on morphological and mechanical changes of Langmuir probes from JET-ILW.*

- *The most important result is the large difference in the hardness value in the tip and the base of LP-5 at side A, 5.4 GPa versus 8.8 GPa, respectively.*

- *The differences in hardness on the base and tip of probe 1, measured on the A-side, were small, which is expected since the probe was placed next to stack A.*

Further plans

- Nanoindentation of probe No. 3.
- FIB cross-sections to assess the grain size in individual zones of LPs.
- Nanoindantaion at higher load.

Thank you for your attention

FIB cross-sections as a good tool for grain size assessment

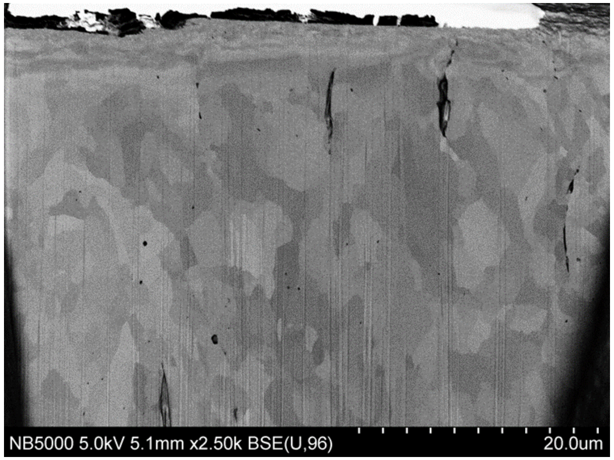

SEM images of the sub-surface structure of FTU molybdenum tile

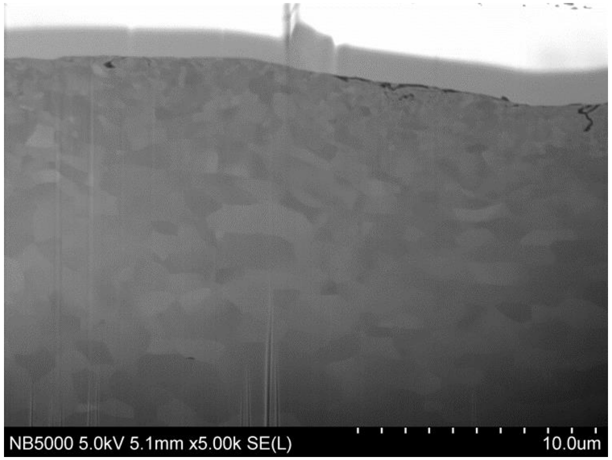

SEM images of the sub-surface structure of Mo sheet.

Surface morphology of other probes

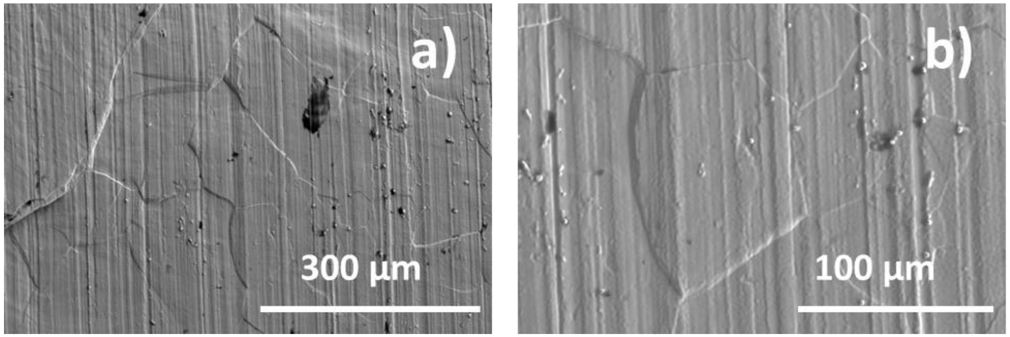

SEM images of the overheated part of the tip surface, LP-26 from Module 16BW, divertor Tile 6.

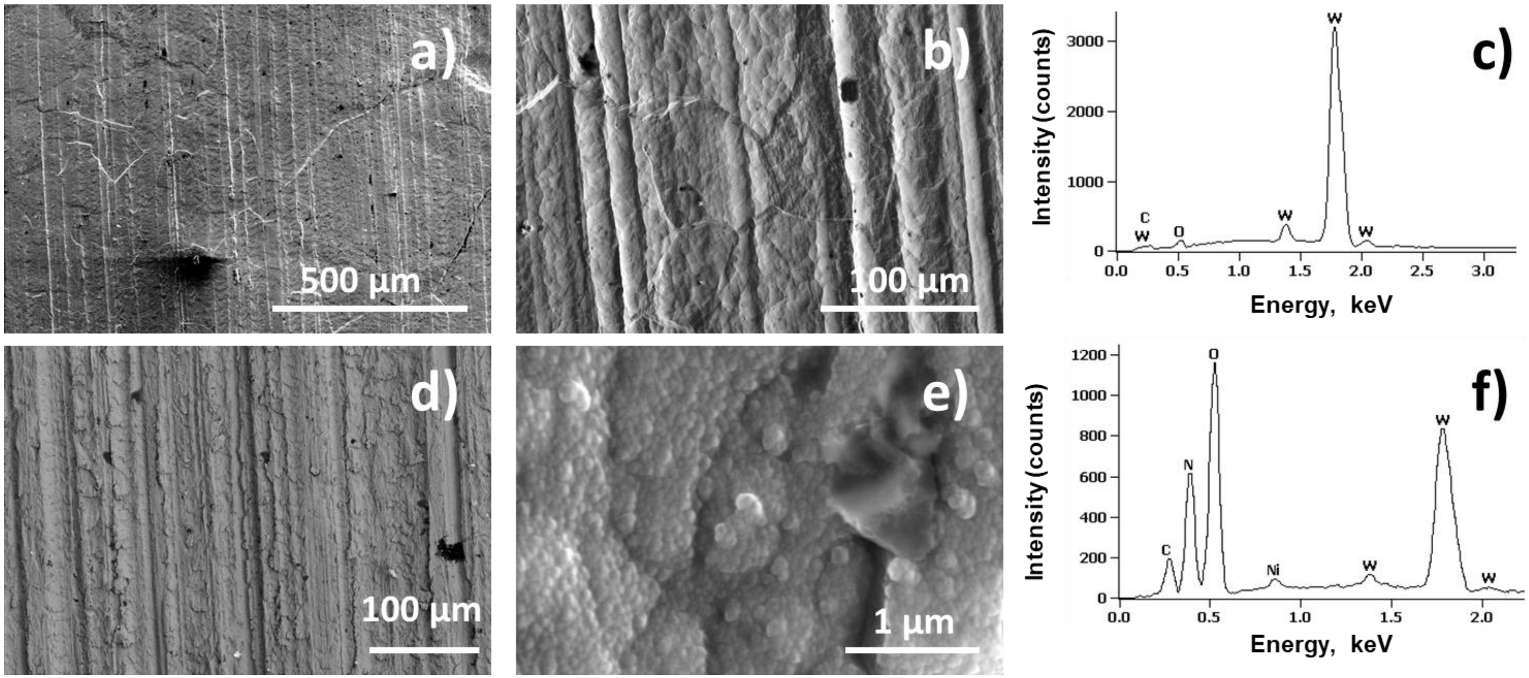

SEM images of the overheated part of tip surface (a)–(b) and support structure (d)–(e) together with the corresponding EDX spectra; results are for LP-5 from Module 16IN, inner divertor Tile 3.